Allosteric Modifiers of Hemoglobin. 2. Crystallographically Determined Binding Sites and Hydrophobic Binding/Interaction Analysis of Novel Hemoglobin Oxygen Effectors

Fred C. Wireko, Glen E. Kellogg, and Donald J. Abraham*

Department of Medicinal Chemistry, Medical College of Virginia/Virginia Commonwealth University, Richmond, Virginia 23298-0581. *Received August 20, 1990*

The protein-bound conformations of six new allosteric effectors similar to bezafibrate that markedly decrease the oxygen affinity of hemoglobin have been determined by X-ray crystallography. Comparisons are made with the bound conformations of three urea analogues reported by Lalezari, Perutz, and co-workers. All six new molecules bind at the same site previously observed for bezafibrate and exhibit a wide range of allosteric activity. Unlike the urea derivatives, which show two binding sites for the most potent derivatives, only one of the six new molecules (one with moderate allosteric activity) exhibits a second binding site. A new computer program, HINT (hydrophobic interactions), has been created and utilized to identify the major interactions between small molecules and the protein. The three strongest interactions identified by HINT involve Arg 141α with the acid of the analogues, Lys 99α with the bridging amide carbonyl, and the amide NH of the side chain of Asn 108β with the halogenated aromatic ring.

Introduction

Recently, several groups have reported synthetic agents that right shift the oxygen equilibrium curve of hemoglobin[1-6] (Figure 1). Abraham et al. were the first to report a nonnaturally occurring agent (clofibric acid, CFA, **1**) that decreases the oxygen affinity of hemoglobin.[1] Perutz and Poyart[2] followed with a more potent allosteric inhibitor, bezafibrate (BZF, **2**). Lalezari and co-workers[3-5] discovered that urea analogues (**3**) of bezafibrate were even more potent allosteric effectors, but their interest as useful clinical agents was limited because of inactivity at physiological concentrations of serum albumin.

In the accompanying contribution[6] we reported the structure–activity relationships of three new isomeric series of compounds that are allosteric effectors of hemoglobin. The new molecules differ in structure from the antilipdemic agent bezafibrate by the elimination of one methylene unit that bridges the aromatic rings. The atoms in the amide bridge of the new derivatives were systematically rearranged as follows: $-NHCOCH_2-$ (**4**), $-CONHCH_2-$ (**5**), and CH_2CONH- (**6**). Compounds in all three series exhibited stronger allosteric effector action than bezafibrate. The structure–activity analysis[6] indicated that the most potent series of the new compounds ($-NHCOCH_2-$) contained the amide nitrogen next to the halogenated aromatic ring. The two most active agents from the $-NHCOCH_2-$ series are the most potent reported to date and maintain their allosteric activity in whole blood.[6] Although the new compounds as well as **2** and **3** are similar structurally, they exhibit a wide range of interesting allosteric activity.

In order to determine the stereochemical basis for the difference in activity that arises from the location of the atoms in the amide bridge, we have crystallized six of the new compounds from two of the three new series ($-NHCOH_2-$ bridge, **4a–c**; $-CONHCH_2-$ bridge, **5a–c**) with human deoxyhemoglobin, collected X-ray diffraction data, and calculated difference electron density maps which yielded the experimental atomic coordinates for each agent in its binding site.

We also have created and employed a new computer program, HINT[7] (hydrophobic interactions), for quantifying and visualizing hydrophobic and polar affinities for individual atoms. HINT also calculates the degree of hydrophobic and polar interaction between atoms in bound drugs or substrates with atoms in the protein. In addition, visualization of the close contacts and interactions between atoms of two of the new derivatives (**4b** and **5b**) with *native* deoxyhemoglobin coordinates through contoured hydrophobicity and hydrophobic interaction map reveals qualitative rationale for the binding modes of these hemoglobin allosteric modifiers and provides an additional tool for structure–activity relationship studies.

Background

Human hemoglobin is an allosteric protein that equilibrates between the deoxy or tense (T) state and the oxy or relaxed (R) state. Arrangement of the four subunits around a molecular twofold axis yields a large central water cavity in the T state and a narrower cavity in the R state. Allosteric effectors that decrease oxygen affinity act by stabilizing the T structure. The natural allosteric effector 2,3-diphosphoglyceric acid (2,3-DPG) stabilizes the T state by formation of salt bridges between the β subunits.[8] Nonnatural allosteric effectors **1** and **2** bind to sites far removed from 2,3-DPG.

Clofibric acid (**1**) binds to several sites in deoxyhemoglobin. X-ray and solution-binding studies show that these sites can be classified as two primary (high occupancy) symmetry-related pairs of sites and two secondary (low occupancy) pairs of sites.[9] The high-occupancy binding sites of **1** were determined by X-ray analysis to be near the surface of the cleft between the α subunits,[2] and the isobutyric acid–phenoxy aromatic ring portion of bezafibrate is located at one of these high-occupancy CFA sites and extends to one of the low-occupancy CFA sites at the interface of the α and β subunits deep in the central water cavity.[10,11] This site as determined from the crystal structure of **2** bound to deoxyhemoglobin[11] will henceforth be referred to as the bezafibrate site. The three urea derivatives (**3a–c**) were also found to bind at the bezafibrate site,[3,5] two of which (**3b**, **3c**) also bound to a second

(1) Abraham, D. J.; Perutz, M. F.; Philips, S. E. V. *Proc. Natl. Acad. Sci. U.S.A.* **1983**, *80*, 324.
(2) Perutz, M. F.; Poyart, C. *Lancet* **1983**, Oct 15, 881.
(3) Lalezari, I.; Rahbar, S.; Lalezari, P.; Fermi, G.; Perutz, M. F. *Proc. Natl. Acad. Sci. U.S.A.* **1988**, *85*, 6117.
(4) Lalezari, I.; Lalezari, P. *J. Med. Chem.* **1989**, *32*, 2352.
(5) Lalezari, I.; Lalezari, P.; Poyart, C.; Marden, M.; Kister, J.; Bohn, B.; Fermi, G.; Perutz, M. F. *Biochemistry* **1990**, *29*, 1515.
(6) Randad, R. S.; Mahran, M. A.; Mehanna, A. S.; Abraham, D. J. *J. Med. Chem.*, preceding paper in this issue.
(7) Kellogg, G. E.; Abraham, D. J. Manuscript in preparation.
(8) Arnone, A. *Nature* **1972**, *237*, 146.
(9) Mehanna, A. S.; Abraham, D. J. *Biochemistry* **1990**, *29*, 3944.
(10) Abraham, D. J.; Kennedy, P. E.; Mehanna, A. S.; Patwa, D.; Williams, F. L. *J. Med. Chem.* **1984**, *27*, 967.
(11) Perutz, M. F.; Fermi, G.; Abraham, D. J.; Poyart, C.; Bursaux, E. *J. Am. Chem. Soc.* **1986**, *108*, 1064.

0022-2623/91/1834-0758$02.50/0

Table I. Crystallographic Data

deoxy Hb	compd added	[compd]/[Hb]	cell dimension				d_{lim},[a] Å	R_{int},[b] %	R_{d-n},[c] %
			a, Å	*b*, Å	*c*, Å	β, deg			
Hb[d]			63.15	83.59	53.80	99.34	1.74	3.6	
	4a	1	63.3	83.7	53.8	99.3	3.0	10.8	13.1
	4b	0.5	63.2	83.5	53.8	99.4	2.8	12.7	14.3
	4c	1	63.2	83.7	53.8	99.4	4.0	6.2	10.2
	5a	3	63.2	83.5	53.7	99.4	3.0	8.2	12.6
	5b	1	63.2	83.5	53.7	99.4	4.0	4.0	6.6
	5c	3	63.3	83.6	53.7	99.4	3.0	6.2	9.2

[a] d_{lim} = (radius)$^{-1}$ of limiting sphere in which data were collected. [b] R_{int} = agreement factor of interactions between Friedel pairs with each set of data: $R_{int} = \sum_{hkl}(|I_{hkl} - I_{\bar{h}\bar{k}\bar{l}}|)/\sum_{hkl}(I_{hkl})$. [c] R_{d-n} = agreement factor of structure amplitudes between native and derivative data: $R_{d-n} = \sum|(|F_d| - |F_n|)|/\sum|F_d|$. [d] Reference 14.

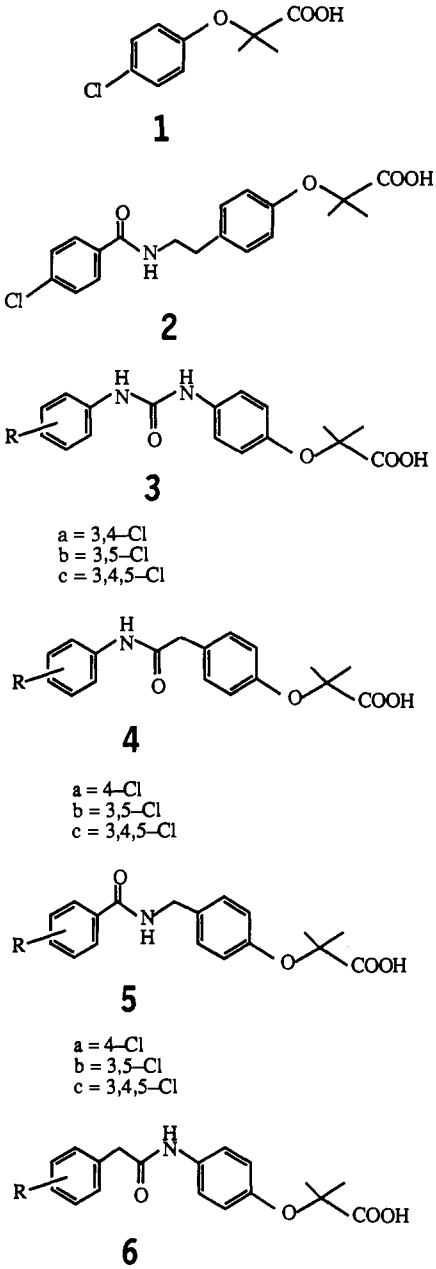

Figure 1. Structures of allosteric effectors.

site[5] that is near another low-occupancy CFA site.[8,9] The latter binding area will be referred to as the secondary site.

Methodology

Preparation of Crystals and Collection of X-ray Data. Hemoglobin was prepared from human blood, and crystals of deoxyhemoglobin (deoxy Hb) were grown according to procedures described by Perutz.[12] Stock solutions of compounds in water were prepared by addition of a slight molar excess of sodium bicarbonate to facilitate dissolution. Next a quantitative concentration of compound was added to a 6 g % solution of deoxy Hb in the glove box. Aliquots of the compound–deoxy Hb were then added to the approximately 2.4 M phosphate buffer to achieve a final concentration of 1 g % in each tube. For all compounds, mountable-sized crystals were obtained from the crystallization tubes within 1 week of setup.

X-ray data were collected for $h,k\pm l$ reflections and their Friedel pairs using ω scans on a Rigaku AFC5R diffractometer equipped with a rotating anode and a 60-cm-long evacuated beam tunnel. Data collection was controlled by TEXRAY software from Molecular Structure Corp.[13] Table I summarizes the X-ray crystallographic details and crystallization conditions for this study. Corrections for radiation damage, absorption, and Lorentz and polarization factors were applied to the data and the intensities from symmetry-related reflections merged to generate a unique set. Structure amplitudes derived from the intensities of the unique set of data were used to calculate difference electron density maps with ($|F_{native+compound}| - |F_{native}|$[14]) as coefficients.

Models of the compounds, initially created using MACROMODEL[15] and minimized using the MM2 force field, were fitted to their respective experimental difference electron density maps with the use of FRODO[16] on an Evans and Sutherland PS390 graphics workstation. The amide moiety for each compound in the calculation was constrained to be planar with the adjacent halogenated aromatic ring. Fits of symmetry-related bound compounds were cross-checked by rotating the model into the difference density at the twofold related site. Atomic coordinates for the bound-drug positions are available as supplementary material.

Hydrophobic Interaction Analysis. Abraham and Leo[17] suggested that hydrophobic fragment constants, reduced to atomic values with inherent bond and proximity factors, could be used to evaluate interactions between small molecules and large molecules. The program HINT[7] was written for this purpose. To demonstrate the utility

(12) Perutz, M. F. *J. Cryst. Growth* **1968**, *2*, 54.
(13) TEXRAY Structure Analysis Package (1985), Molecular Structure Corporation, The Woodlands, TX 77381.
(14) Fermi, G.; Perutz, M. F.; Shaanan, B.; Fourme, R. *J. Mol. Biol.* **1984**, *175*, 159.
(15) Still, W. C.; Mohamadi, F.; Richards, N. G. J.; Guida, W. C.; Lipton, M.; Liskamp, R.; Chang, G.; Hendrickson, T.; DeGunst, F.; Hasel, W. MacroModel V2.5, Department of Chemistry, Columbia University, New York, NY 10027.
(16) (a) Evans, P. Modified Frodo 27 Version E 2.0, April 1985, MRC Laboratory of Molecular Biology, Hills Road, Cambridge CB2 2QH, England. (b) Jones, T. A. *J. Appl. Crystallogr.* **1978**, *11*, 268.
(17) Abraham, D. J.; Leo, A. J. *Proteins: Struct. Funct. Genet.* **1987**, *2*, 130.

of the program, the hydrophobic and polar interactions between compounds 2–5 with the deoxy Hb binding site were examined. HINT calculates a double sum for the total protein/substrate interaction

$$B = \sum\sum b_{ij} = \sum_{i=1}^{\text{protein}} \sum_{j=1}^{\text{drug}} (s_i a_i s_j a_j R_{ij} + r_{ij}) \quad (1)$$

where b_{ij} is a dimensionless "microbinding parameter" specific to the atom pair ij, s is a term representing the normalized solvent accessible surface area, a is the hydrophobic atom constant, and R and r are functions of the distance between atoms i and j. The hydrophobic atom constants were obtained by reduction of Hansch and Leo fragment constants derived from the water–octanol partition coefficient.[18] These atomic constants contain implicit contributions from bond, chain, branch, and polar proximity factors that have been ignored in other approaches. Positive signed atom (or fragment) constants indicate hydrophobic atoms (or fragments) while negative signed constants indicate hydrophilic atoms (or fragments). Atom-based hydrophobic constants are constructed from fragment (group) constants such that (a) the sum of hydrophobic atom constants in a group is consistent with the group's fragment constant; (b) frontier atoms in a group are more important than shielded (central) atoms and are generally maintained at atom values; (c) hydrogens are treated implicitly with united atom types for C, N, O, S; (d) bond, chain, branch, and proximity factors are applied as additive constants, the first three to all eligible atoms while the last to the central atom of polar groups. Partition coefficients (sum of hydrophobic atom constants) for small molecules calculated by HINT are similar to values calculated by Hansch and Leo.[18] Hydrophobic atom constants for nonterminal amino acid residues are computed from the acetyl amide analogues for the residue.[17]

The functional form of the range dependence is described by two terms (R_{ij} and r_{ij}, eq 1). The former scales the hydrophobic atom constant–solvent accessible surface area product with distance, while the second is independent of hydrophobicity and responds only to distance variations. The function R_{ij} for this study was

$$R_{ij} = T_{ij}e^{-r} \quad (2)$$

where T_{ij} is a sign-flip function that recognizes acid–base interactions, and r is the normalized distance between atoms i and j. Interestingly, e^{-r}, where r is the distance in angstroms, is a resonable fit[19] to the Hansch and Leo polar proximity factors[18] for intramolecular through-bond polar–polar interactions. r_{ij}, which adds a Lennard-Jones type potential, was

$$r_{ij} = (A)(\epsilon_{ij})[(r_{vdw}/r)^{12} - 2(r_{vdw}/r)^{6}] \quad (3)$$

Here A is a scaling factor between the exponential (eq 2) and Lennard-Jones terms, defined by Levitt[20] and Perutz and Levitt,[21] ϵ_{ij} is the depth of the Lennard-Jones potential well, and r_{vdw} is the sum of van der Waals radii for atoms i and j.

Superimposition of a three-dimensional grid of test atoms over the molecule or region of interest allows the calculation of a hydrophobic field. The test atoms are assumed to have solvent-accessible surface areas, hydrophobic atom constants, and other parameters set to unity. Maps displaying graphically the polar and hydrophobic interactions between the protein and substrate–drug are calculated by an adaptation of eq 4;

$$A_t = \sum\sum[(s_i a_i R_{jt})(s_j a_j R_{jt}) + r_{it}r_{jt}] \quad (4)$$

where A_t is the map value at the test point t, and R_{it}, R_{jt}, r_{it}, and r_{jt} are the distance functions between atoms i (or j) and the test point. Hydrophobicity and interaction maps were contoured using FRODO and displayed on the E&S PS390 graphics station.

Table II. Allosteric Activity for Right-Shifting Agents[a]

compd	P_{50}^{d}/P_{50}^{c} [b]	compd	P_{50}^{d}/P_{50}^{c} [b]
2	1.74 (6)	**4b**	4.32 (8)
3a	1.77	**4c**	3.17 (9)
3b	3.62 (9)	**5a**	2.58 (9)
3c	2.57 (7)	**5b**	2.48 (5)
4a	2.79 (4)	**5c**	2.13 (8)

[a] All studies were carried out at 2.7 mM hemoglobin concentration in the presence of 10 mM drug concentration using 50 mM HEPES buffer of pH 7.4. [b] P_{50}^{d}/P_{50}^{c} is the ratio of the oxygen pressures in mmHg between Hb–compound and compound-free Hb (control) solutions at which 50% oxygen saturations are respectively attained. Standard deviations of the averaged P_{50} ratios are shown in parentheses.

Biological Evaluation

The six molecules chosen for detailed crystallographic and hydrophobic binding (HINT) analysis are derivatives of two classes of compounds that differ only by the linkage order of the amide moiety between the two phenyl rings (i.e. **4a–c** vs **5a–c**). The biological results for these and related compounds were described in detail in the previous communication.[6] Table II briefly summarizes the results for compounds compared in this study. The activities in Table II are expressed as a ratio $P_{50}^{drug}/P_{50}^{control}$, where the P_{50} value is the partial pressure of oxygen (in mmHg) that results in 50% oxygenation of hemoglobin.

Table II reveals that all three compounds in series 4 are more active than any derivative in series 5. The 3,5-dichloro derivative **4b** shows the largest allosteric effector activity of all agents studied thus far. The new series and the ureas show a wide range of allosteric effects despite close structural similarities. These differences prompted the present study.

Results

Binding Sites. All six new molecules have at least one pair of symmetry-related binding sites. One of the pair is near Lys 99α_1 in the central water cavity of deoxyhemoglobin in approximately the same location found for bezafibrate[11] and the urea derivatives.[3,5] The symmetry-related binding site is near Lys 99α_2. Either of these symmetry-related sites can be described in terms of a "niche" formed by the van der Waals radii of the protein around the bound compounds (Figure 2). The six new molecules bound at the bezafibrate site all fit well within the pocket defined by the interfaces between the α_1, α_2, and β_1 hemoglobin subunits.

One derivative (**5a**) has a second pair of symmetry-related sites near Arg 104β where clofibric acid (1) and the urea derivatives **3b** and **3c** have been shown to bind. Figure 3 shows the superposition of **5a**, **3b**, and **3c** with the van der Waals radii of the protein. This site does not appear to be a well-defined pocket, and binding of the acids here is probably due to strong interactions with the charged Arg side chains.

Conformations of Bound Compounds. The analogues were grouped for study of the experimentally determined bound conformations according to their degree of halo-

(18) Hansch, C.; Leo, A. J. *Substituent Constants for Correlation Analysis in Chemistry and Biology*; J. Wiley and Sons: New York, NY, 1979; pp 1–339.
(19) Fauchere, J. L.; Quarendon, P.; Kaetterer, L. *J. Mol. Graphics* **1988**, *6*, 203.
(20) Levitt, M. *J. Mol. Biol.* **1983**, *168*, 595.
(21) Levitt, M.; Perutz, M. F. *J. Mol. Biol.* **1988**, *201*, 751.

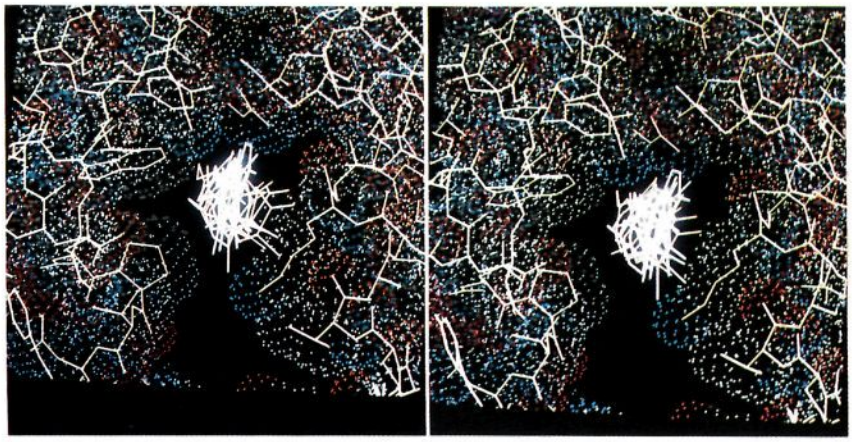

Figure 2. Stereoview of the bezafibrate site with superposition of the allosteric effectors. Lys 99α, which bisects the allosteric effectors, is shown in the lower right foreground. This primary binding site "niche" is depicted using 80% van der Waals radii for the protein atoms.

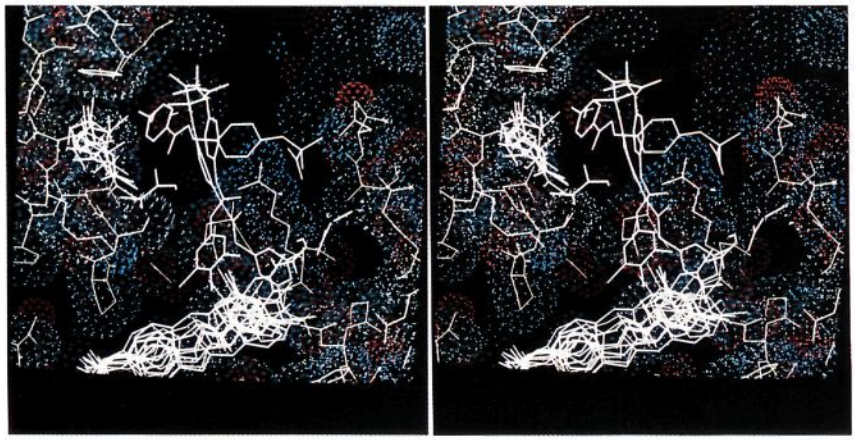

Figure 3. Stereoview of the secondary site with superposition of the allosteric effectors. This fairly loose "niche" is defined by binding near Arg 104β. Compound **5a** is located above Arg 104β and horizontal while urea derivatives **3b** and **3c** are to the left and perpendicular to Arg 104β. The superposition of the allosteric effectors bound to the primary bezafibrate binding sites can be seen at the lower center and upper left of the figure. The secondary "niche" is depicted using 80% van der Waals radii for the protein atoms.

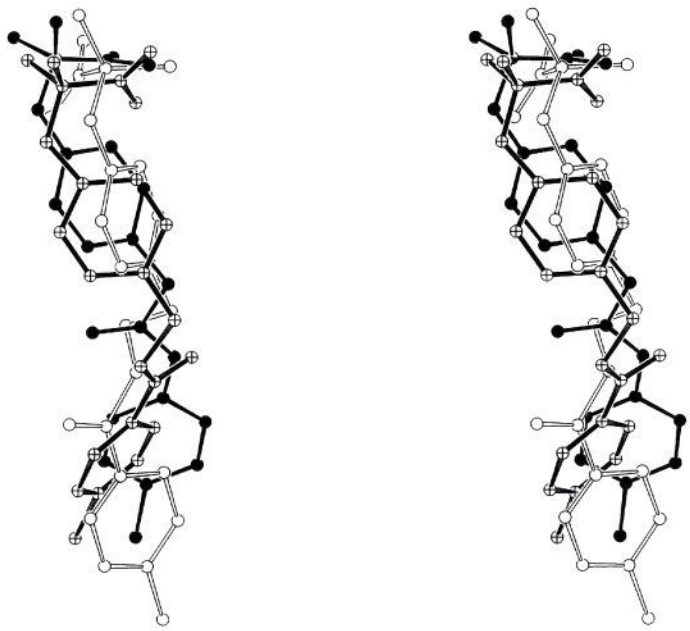

Figure 4. Stereoview overlay of the X-ray determined conformations for the *p*-chloro compounds **2** (○), **4a** (●), and **5a** (⊕) at the bezafibrate site. Compound **2** is longer than **4a** and **5a**, which probably accounts for the conformational differences of **2** compared to **3**, **4**, and **5**. The amide oxygens of **2** and **4a** are parallel and point directly toward the ammonium ion (NZ) of Lys 99α side chain. The amide oxygen of **5a** is pointed in the opposite direction (see text for further details).

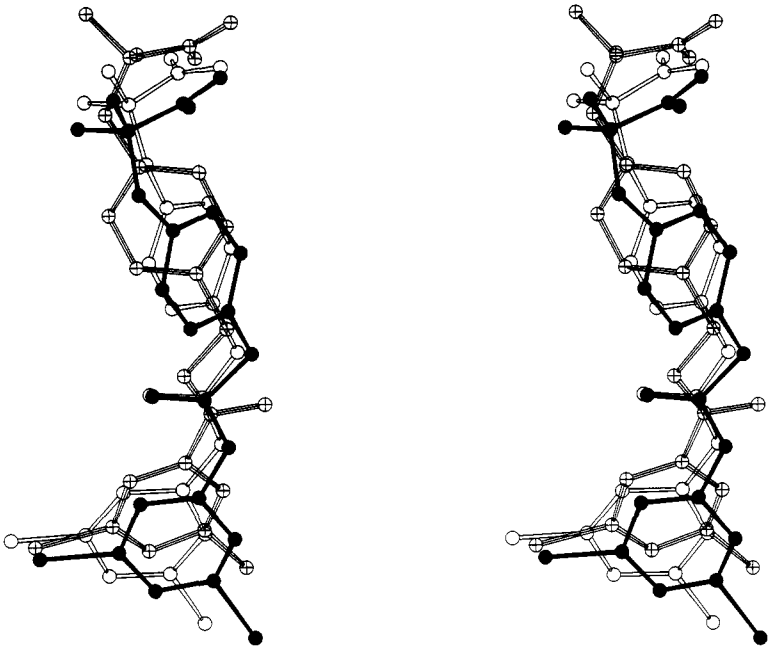

Figure 5. Stereoview overlay of the X-ray determined conformations for the 3,5-dichloro compounds **3b** (○), **4b** (●), and **5b** (⊕) at the bezafibrate site. The amide oxygens of **3b** and **4b** are virtually superimposed and point directly toward the ammonium ion (NZ) of Lys 99α side chain. The amide oxygen of **5b** is pointed in the opposite direction (see text for further details).

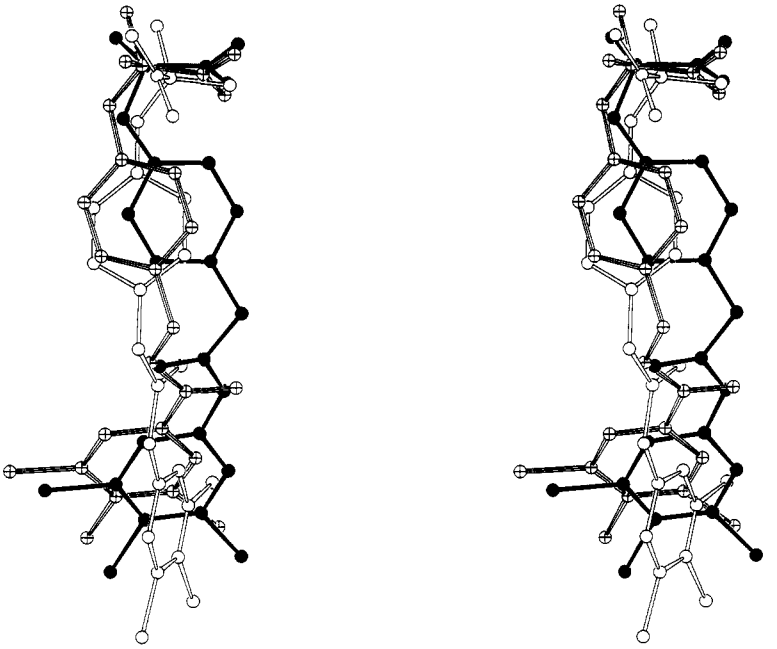

Figure 6. Stereoview overlay of the X-ray determined conformations for the 3,4,5-trichloro compounds **3c** (○), **4c** (●), and **5c** (⊕) at the bezafibrate site. The acid group of **3c** is directed opposite to the acids of all other derivatives which point toward Arg 141α. The amide oxygens of **3c** and **4c** are pointed toward the ammonium ion (NZ) of Lys 99α side chain. The amide oxygen of **5c** is pointed in the opposite direction to **4c** (see text for further details).

genation: the *p*-chloro compounds (**2**, **4a**, **5a**, Figure 4), the 3,5-dichloro compounds (**3b**, **4b**, **5b**, Figure 5), and the 3,4,5-trichloro compounds (**3c**, **4c**, **5c**, Figure 6). Conformations of compounds bound at the symmetry related Lys 99α_2 site are similar in detail and are not shown. Superposition of compounds that bind to the secondary site (**3b**, **3c**, and **5a**) near Arg 104β_1 is depicted in Figure 7.

Hydrophobic–Hydrophilic Analysis. First we examined via HINT the hydrophobicity environments of the protein and drug separately, and then calculated the hydrophobic interactions between bound compounds **2**–**5** with deoxyhemoglobin. Since positive hydrophobic atom constants indicate affinity for a hydrophobic environment, negative hydrophobic atom constants indicate an affinity for a polar environment. Thus, these constants supply micro-thermodynamic information that can be used to estimate polar as well as nonpolar interactions between species.

We chose compounds **4b** and **5b** (one from each new class) to illustrate contoured HINT maps (Figure 8). The areas of highest hydrophobicity (e.g. rings, aliphatic carbons, etc.) are shown in blue, while the hydrophilic (polar) regions (e.g. COO^-, C=O, NH_3^+, etc.) are shown in red. A similar map for deoxyhemoglobin at the bezafibrate Lys 99α_1 site is shown in Figure 9 with a similar color scheme.

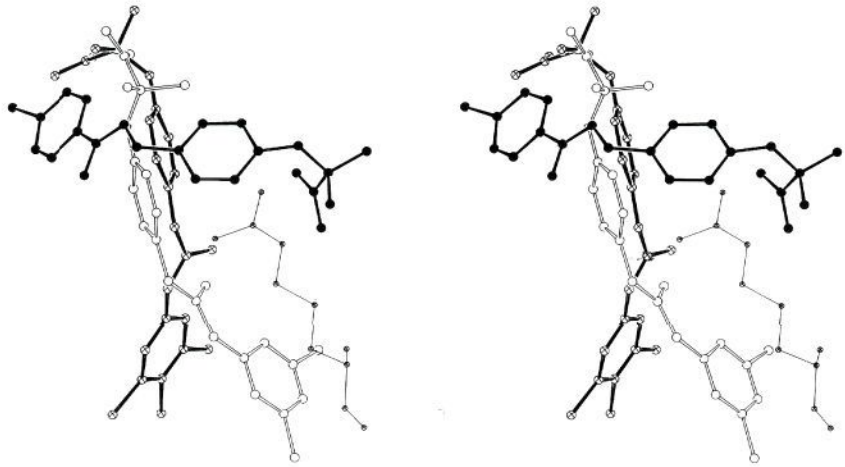

Figure 7. Stereoview overlay of the X-ray determined conformations for the **3b** (○), **3c** (⊕), and **5a** (●) at the secondary Arg 104β site. Allosteric effectors **3b** and **3c** are located to the right of Arg 104β while **5a** is above and to the left of Arg 104β (see text for details of interaction with the primary bezafibrate site).

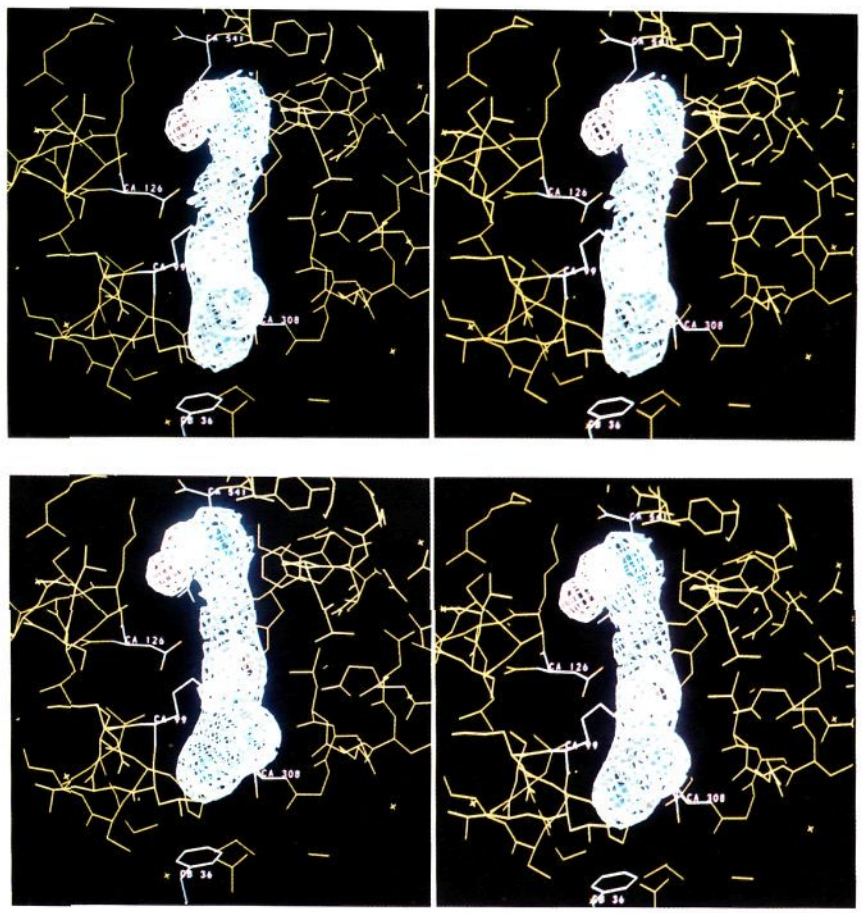

Figure 8. HINT atomic hydrophobicity field contours for **4b** (top) and **5b** (bottom) bound to the bezafibrate site. The red contours indicate strong polar regions and the blue contours signify strong hydrophobic regions. The lighter blue and red contours indicate lesser polar and hydrophobic regions, respectively.

The composite small molecule–protein complex interactions using HINT will be illustrated and discussed below.

Discussion

Binding at the Primary Bezafibrate Site. As was shown above, the four structural classes (**2**, **3**, **4**, **5**) all bind in a similar orientation in a relatively well defined pocket bisected by Lys 99α (Figure 2). There are, however, significant differences in bound conformations among the series that suggest an interesting variety of small molecule–protein interactions giving rise to the differences in allosteric activity observed.

HINT indicates three regions of strong interaction. The specific details of the small molecule–protein interactions are discussed sequentially below and are organized by functional groups of the small molecules. Numerical HINT results are set out in Table III for the four most significant binding–promoter interactions between deoxyhemoglobin

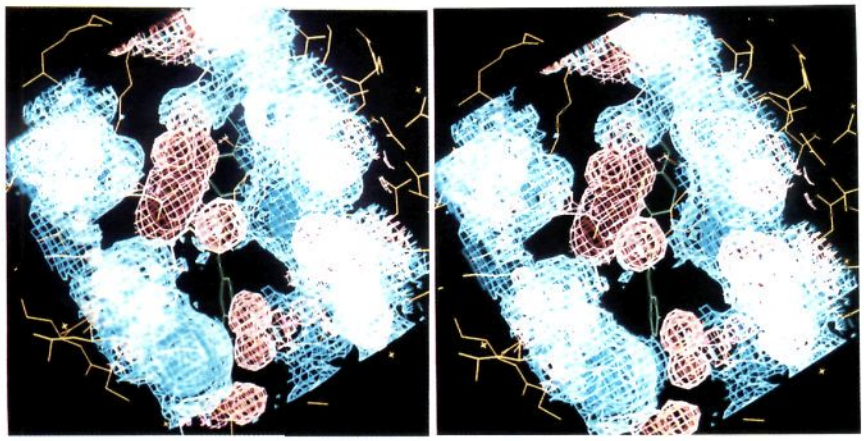

Figure 9. HINT atomic hydrophobicity field contours for protein atoms at the bezafibrate site. The red contours indicate strong polar regions and the blue contours signify strong hydrophobic regions. The lighter blue and red contours indicate lesser hydrophobic and hydrophilic regions, respectively. Compound **4b** can be seen (light green) in the right center of the cavity. The large red sphere in the center of the cavity (foreground) arises from the ammonium ion (NZ) of Lys 99α. The large red contours to the left of Lys 99α are from the carboxy terminus and the guanidinium ion of Arg 141α and Asp 126α. The side chain amide of Asn 108β (red pair of spheres) that interacts with the halogenated aromatic ring of **4b** is seen in the lower right portion of the figure.

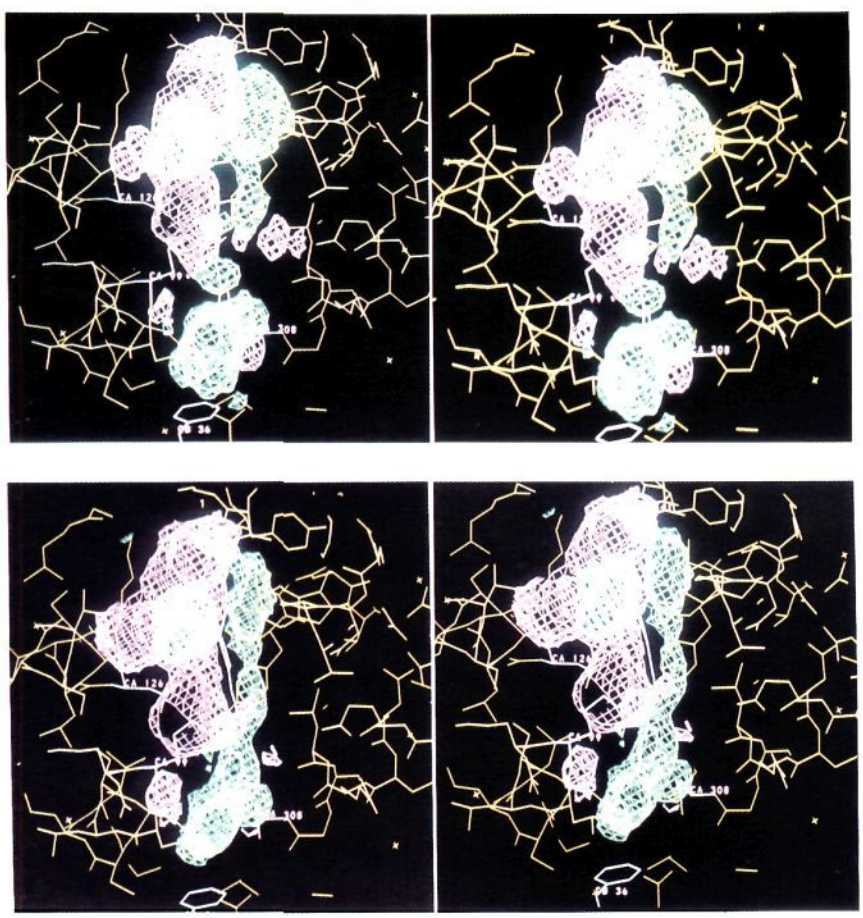

Figure 10. HINT interaction contours between **4b** (top figure), **5b** (bottom figure), and the protein as calculated by eq 1–4 (see text). The green contours indicate positive interactions between **4b** and **5b** with the protein, and the purple contours indicate unfavorable interactions. In general, favorable interactions run along the right side of the allosteric effectors and negative interaction are seen on the other side. The lower portions of the figures indicate a large positive interaction of the halogenated aromatic ring with the protein. The green trapezoidal contour (top figure) on the ammonium ion of Lys 99α arises from the positive interaction of Lys 99α NZ with the amide oxygen of the derivatives from **4** and not **5**. The positive interaction contours at the top of the figure arises from the interaction of Arg 141α with the carboxylate oxygens of the allosteric effectors (see text for general discussion of the negative interactions).

and compounds **2**–**5**. Tabulated are the average atom–atom distance in the interaction, r_{ij}, and the sum of the individual atom–atom interactions, $\sum\sum b_{ij}$. The important hydrophobic–hydrophilic interactions between the bound molecules and the deoxyhemoglobin protein are pictorially represented by Figure 10 for **4b** and **5b**. The contour maps

Table III. Selected Hydrophobic–Polar Interactions between Bound Drug Atoms (Positions Determined by X-ray) and Deoxyhemoglobin Atoms (Native Structure)

	interaction				
	atoms				
compd	i[a]	j[b]		r_{ij},[c] Å	$\sum\sum b_{ij}$[d]
2	O2,O3	Arg 141α_2	NH1, NH2	6.42	182[e]
	O18	Lys 99α_1	NZ	4.68	66[f]
	C19–C24	Asn 108β_1	ND2	3.38	157
	Cl25	Phe 36α_1	CE2, CZ, CE1	2.98	97
3a	O2,O3	Arg 141α_2	NH1, NH2	5.02	850
	O16	Lys 99α_1	NZ	6.09	16[f]
	C18–C23	Asn 108β_1	ND2	3.32	163
	Cl24	Phe 36α_1	CE2, CZ, CE1	3.26	71
3b	O2,O3	Arg 141α_2	NH1,NH2	4.82	783
	O16	Lys 99α_1	NZ	4.70	65[f]
	C18–C23	Asn 108β_1	ND2	4.39	69
	Cl25	Phe 36α_1	CE2, CZ, CE1	3.84	39
3c	O2,O3	Arg 141α_2	NH1, NH2	6.49	152[e]
	O16	Lys 99α_1	NZ	5.29	36[f]
	C18–C23	Asn 108β_1	ND2	3.54	124
	Cl25	Phe 36α_1	CE2, CZ, CE1	6.08	4
4a	O2,O3	Arg 141α_2	NH1, NH2	5.11	651
	O16	Lys 99α_1	NZ	4.88	54[f]
	C18–C23	Asn 108β_1	ND2	4.25	72
	Cl24	Phe 36α_1	CE2, CZ, CE1	4.66	17
4b	O2,O3	Arg 141α_2	NH1, NH2	4.43	1138
	O16	Lys 99α_1	NZ	4.70	65[f]
	C18–C23	Asn 108β_1	ND2	3.76	123
	Cl25	Phe 36α_1	CE2, CZ, CE1	3.84	40
4c	O2,O3	Arg 141α_2	NH1, NH2	4.29	1463
	O16	Lys 99α_1	NZ	5.28	36[f]
	C18–C23	Asn 108β_1	ND2	4.01	101
	Cl25	Phe 36α_1	CE2, CZ, CE1	4.54	19
5a	O2,O3	Arg 141α_2	NH1, NH2	4.77	893
	O17	Lys 99α_1	NZ	7.03	6[g]
	C18–C23	Asn 108β_1	ND2	4.12	58
	Cl24	Phe 36α_1	CE2, CZ, CE1	5.33	9
5b	O2,O3	Arg 141α_2	NH1, NH2	4.69	942
	O17	Lys 99α_1	NZ	7.10	6[g]
	C18–C23	Asn 108β_1	ND2	4.16	69
	Cl25	Phe 36α_1	CE2, CZ, CE1	4.95	13
5c	O2,O3	Arg 141α_2	NH1, NH2	4.30	1417
	O17	Lys 99α_1	NZ	6.73	8[g]
	C18–C23	Asn 108β_1	ND2	4.80	48
	Cl26	Phe 36α_1	CE2, CZ, CE1	5.06	11

[a] Atom definitions for compounds: O2, O3 are the isobutyric carboxylate oxygens; O16, O17, or O18 is the amide oxygen; C18–C23 or C19–C24 are the carbons in the halogenated ring; Cl24, Cl25, or Cl26 is the *p*-Cl for **2**, **4a**, and **5a** or the *m*-Cl for **3a–c** **4b,c**, and **5b,c**. [b] Atom definitions for protein: atoms and residues are named by Brookhaven Protein Data Bank conventions. [c] Average of distances between atoms i and j. [d] Sum of interactions between atoms i and j (see eqs 1–3 where $A = 50$ and other variables as defined in text). b_{ij} should be regarded as a dimensionless scalar. [e] Acid group of compound as determined in X-ray structures is turned away from guanidinium group of Arg 141α_2. [f] At $r_{ij} = 2.8$ Å, $b_{ij} = 430$; Lys 99α_1 should be able to come within 3 Å of the amide oxygen. Thus, in the bound complex this interaction would likely be the second most important. [g] Amide carbonyl points away from Lys 99α_1; significant improvement in this interaction is unlikely in the bound complex.

were calculated using eq 4, and the maps were contoured and displayed using FRODO.

a. The Phenoxy Aromatic Ring and Isobutyric Acid Group. The aromatic phenoxy rings for nearly all of the new compounds (**4** and **5**) are approximately parallel (Figures 4–6), as was seen for **3b** and **3c** by Lalezari et al.[3,5] Compound **4b** appears to be slightly skewed from the ring plane defined by the other compounds. Bezafibrate (**2**), probably because of its longer inter-ring chain, does not overlap well with **3–5** in the phenoxy ring or isobutyric acid regions.

The isobutyric acid group of compounds **3–5** fit within a relatively small volume (Figures 4–6). The carbons of the acid groups are, in fact, within 2 Å of one another. Planes defined by the acid groups are, in a general sense, parallel and aligned in a similar direction. The sole exception is **3c**, where the methyls of the isobutyric group align with the acid oxygens of the other compounds.[5]

These consistent positions and orientations of the small molecule isobutyric acid groups suggest a strong interaction with a residue or residues in the protein. Figure 10 and Table III from HINT show that there is an interaction between the two oxygens of the isobutyric acid group and two of the nitrogens of the guanidinium group of Arg 141α, giving rise to a pair of hydrogen bonds. In fact, Table III suggests that this interaction, for all compounds, is the most significant with respect to binding. This interaction is shown in Figure 10 as a green contour encompassing this region. Negative interactions in this region (purple contours) for the most part arise from hydrophobic–hydrophilic interactions between the acids of the small molecules and the Arg 141α carboxy terminus. Also contributing a negative interaction in this region is the hydrophilic Asp 126α, which is in close proximity to the phenoxy aromatic ring. The interaction contours and interation sums (Table III) calculated by HINT are from convolution of *native* protein conformation with the experimentally determined (crystallography) bound small molecule conformation. Because it is known that there can be significant rearrangement of protein structure upon binding of sub-

strates,[22,23] it is not unreasonable to expect that in the bound molecule–protein complex there would be optimization of protein–small molecule interactions. There is, in fact, evidence of protein movement in the experimental X-ray difference electron density maps. Extensive calculations are presently being conducted to obtain energy-minimized protein and allosteric effector positions; however at this stage of structure–activity analysis (SAR) the native protein coordinates were used to give unbiased and entirely *experimental*-based comparison between compounds.

b. The Amide Oxygen and Lys 99α. The inversion of the amide linkage (i.e. between series 4 and 5) results in a reversal of the direction of the amide oxygen of the bound molecules. The amide carbon–oxygen bonds in series 4 are directed parallel to those of bezafibrate (2) and the urea analogues **3a** and **3b**, while the carbon–oxygen bonds in series 5 are directed in an opposite sense. From the hydrophobic interaction contours of Figure 10 (top) it can be seen that the amide oxygens directed as in **2**, **3a**, **3b**, and 4 are in excellent proximity for interaction with the terminal side chain ammonium atom NZ of Lys 99α. In contrast, Figure 10 (bottom) shows that the amide oxygens directed as in **5** are less able to interact with Lys 99α. The apparent importance of the Lys 99α–amide oxygen interaction is somewhat diluted (Table III) by the use of nonoptimized protein coordinates, but close approach of the two interacting atoms to ca. 2.8 Å would increase by b_{ij} by 1 order of magnitude. In general, the crystallographically determined positions of Lys side chain atoms have relatively high temperature factors, indicating substantial rotational and translational freedom. It is interesting to note, however, that the allosteric agents with the amide oxygen orientation toward NZ of Lys 99α are generally more potent than those agents with the amide orientation away from Lys 99α. The electronic and steric reasons that dictate the position of the amide bond orientation in the bound states are, as yet, unknown.

c. The Halogenated Aromatic Ring. The halogenated aromatic rings for the compounds with only one symmetry-related pair of binding sites (**2**, **3a**, 4, **5b**, **5c**) overlap quite well and are close to parallel (Figures 4–6). For the other compounds (**3b**, **3c**, **5a**) that also occupy secondary binding sites there are a variety of orientations for the halogenated aromatic rings, probably mandated by interaction(s) between the molecules binding in the primary and secondary sites. Also interesting is the alignment of chlorines in the 3-position (left in Figures 5 and 6) of the rings for many of the compounds. HINT analysis suggests two small molecule–protein interactions are primarily responsible for the ring orientation. The first, between ND1 of ASN 108β and the ring carbons is a Lewis acid–base interaction that has been described by Perutz et al.,[11] Levitt and Perutz,[21] and Burley and Petsko.[24] The second interaction, which may account for the alignment of chlorines in the 3-position of the rings is a hydrophobic–hydrophobic interaction between the ring of Phe 36α and the small molecule halogenated rings. Bezafibrate (**2**) is longer than all other derivatives, and its chlorine atom extends more toward Phe 36α with probable steric hindrance in binding. Note, however, that steric and electronic considerations dictated by the presence of molecules at the secondary binding site may take precedence over these two small molecule–protein interactions.

Binding at the Secondary Site. A second symmetry-related pair of binding sites for four aromatic halogenated phenoxy acids has been observed. Compounds **1**, **3b**, **3c**, and **5a** bind at this site. We refer to this as a "secondary" site since it has never been observed in the absence of binding at the primary bezafibrate site. This site is located near the Arg 104β side chain which stretches across the central water cavity. Figure 3 shows the van der Waals surface area of the protein in the vicinity of this site. It is clear from this, and the small molecule overlap shown in Figure 7, that there is a greater diversity of orientation for molecules binding at this site. It is not yet clear, however, what protein residues or intermolecular interactions with molecules bound at the primary site influence the secondary binding site orientation. It is noteworthy that while the aromatic rings at the primary and secondary sites for the two urea derivatives **3b** and **3c** tend to align parallel,[5] suggesting a π–π interaction between them; derivative **5a** has the halogenated aromatic rings from the two sites perpendicular to each other reminscent of the edge-to-face interactions between aromatic rings reported previously.[11,25]

The fact that **4b**, which binds only to the primary site, is more active than the urea analogue **3b**, which binds to both sites, appears to eliminate a direct correlation between the number of occupied sites and potency for allosteric activity. The only structural difference between **3b** and **4b** is the replacement of a –NH– with a $-CH_2-$. Elucidation of the role of the second site in allosteric regulation of hemoglobin requires further investigation.

Relation between HINT Results and Biological Activity. A few comments must be made in regard to predicting biological activity using an SAR approach such as HINT. First, for de novo predictions, an uncertainty arises when evaluating drug–protein interactions due to protein side chain movement in bound-drug complexes. This is especially apparent in comparisons between compounds from different classes of molecules. Second, binding affinity may not always be directly related to biological activity. This distinction is the basis of the concept of "intrinsic activity", and is discussed in the next section. Third, HINT is a *qualitative* tool for estimation of binding in much the same way that GRID[26] gives qualitative energies. For example, in comparing crystallographically determined binding sites for 10 different compounds, it is difficult to perceive which interactions might be key and subject to modification. HINT suggested which of the protein–drug interactions in the deoxyhemoglobin complexes were the most important, and further suggested their relative strengths. New synthetic agents based on those HINT criteria are currently under investigation.

The four $\sum\sum b_{ij}$ values listed for each compound in Table III are the four most significant binding-promoting interactions in the deoxyhemoglobin–drug complexes. Table III demonstrates that the compounds with higher activity (Table II) have generally larger $\sum\sum b_{ij}$ parameters. Compound **4b** has among the highest $\sum\sum b_{ij}$ parameters for all four interactions and has the highest biological activity.

Solution Binding vs X-ray Binding. A study comparing the solution binding constants with X-ray interactions for these analogues is under way in our laboratories.

(22) Quiocho, F. A.; Bethge, P. H.; Lipscomb, W. N.; Studebaker, J. F.; Brown, R. D.; Koenig, S. H. *Cold Spring Harbor Symp. Quant. Biol.* **1971**, *36*, 561.
(23) Miller, M.; Schneider, J.; Sathyanarayana, B. K.; Toth, M. V.; Marshall, G. R.; Clawson, L.; Selk, L. M.; Kent, S. B. H.; Wlodawer, A. *Science* **1989**, *246*, 1149.
(24) Burley, S. K.; Petsko, G. A. *FEBS Lett.* **1986**, *201*, 751.
(25) Burley, S. K.; Petsko, G. A. *Science* **1985**, *229*, 23.
(26) Goodford, P. J. *J. Med. Chem.* **1985**, *28*, 849.

With the solution binding constants in hand, we should be able to determine if the allosteric activity differences observed are solely due to the differences in the interactions observed in the X-ray studies or due to the intrinsic nature (activity) of the compounds to shift the allosteric equilibrium. It is possible that two molecules with very similar or identical binding constants can differ markedly in their allosteric effector capabilities. The concept that a molecule's biological effect might arise not only from its binding affinity but incorporate a potency factor (called intrinsic activity) has been well established in receptor research.[27]

Acknowledgment. We gratefully acknowledge grant support for these studies from the National Institutes of Health NIH HLBI-1 RO1 H1 32793. The authors thank Drs. M. F. Perutz and G. Fermi for helpful discussions and for the coordinates of the urea derivatives in series **3**.

Supplementary Material Available: Orthogonal coordinates of compounds **4a–c** and **5a–c** with reference to human deoxyhemoglobin coordinates after applying the translation 16.61, 13.72, 37.65 to *X*, *Y*, and *Z*, respectively, in accordance with the matrix information in the Brookhaven Protein Data Bank (7 pages). Ordering information is given on any current masthead page.

(27) Ariens, E. J. *Molecular Pharmacology*; Academic Press: New York, NY, 1964; Vol. 1 (Vol. 3 of Medicinal Chemistry—a series of monographs), pp 136–144, 183–191.

Synthesis of High Specific Activity (+)- and (−)-6-[^{18}F]Fluoronorepinephrine via the Nucleophilic Aromatic Substitution Reaction

Yu-Shin Ding,* Joanna S. Fowler, S. John Gatley, Stephen L. Dewey, and Alfred P. Wolf

Chemistry Department, Brookhaven National Laboratory, Upton, New York 11973. *Received August 6, 1990*

The first example of a no-carrier-added ^{18}F-labeled catecholamine, 6-[^{18}F]fluoronorepinephrine (6-[^{18}F]FNE), has been synthesized via nucleophilic aromatic substitution. The racemic mixture was resolved on a chiral HPLC column to obtain pure samples of (−)-6-[^{18}F]FNE and (+)6-[^{18}F]FNE. Radiochemical yields of 20% at the end of bombardment (EOB) for the racemic mixture (synthesis time 93 min), 6% for each enantiomer (synthesis time 128 min) with a specific activity of 2–5 Ci/μmol at EOB were obtained. Chiral HPLC peak assignment for the resolved enantiomers was achieved by using two independent methods: polarimetric determination and reaction with dopamine β-hydroxylase. Positron emission tomography (PET) studies with racemic 6-[^{18}F]FNE show high uptake and retention in the baboon heart. This work demonstrates that nucleophilic aromatic substitution by [^{18}F]fluoride ion is applicable to systems having electron-rich aromatic rings, leading to high specific activity radiopharmaceuticals. Furthermore, the suitably protected dihydroxynitrobenzaldehyde 1 may serve as a useful synthetic precursor for the radiosynthesis of other complex ^{18}F-labeled radiotracers.

Positron emission tomography (PET) is an in vivo imaging modality which measures the spatial and temporal distribution of positron emitter labeled compounds and their labeled metabolites in a volume element of living tissue.[1] Although the heart has been extensively studied with PET, it has been examined mainly from the perspective of assessing perfusion and substrate metabolism.[2] However, the neuronal integrity of the heart is also important in assessing cardiac physiology and pathophysiology[3,4] and there has been an interest in probing this function in vivo by using external imaging beginning with the synthesis of [^{11}C]norepinephrine in the early 1970's.[5,6] Recently, interest has intensified with the development of [^{18}F]fluorometaraminol[7] and [^{11}C]*m*-hydroxyephedrine.[8] Both compounds are metabolically stable false neurotransmitters for norepinephrine. These tracers share the same uptake and storage mechanisms as norepinephrine and provide excellent images of the neuronal distribution in dog heart,[9,10] and human heart.[11] Ring-fluorinated catecholamines such as 6-fluoronorepinephrine[12,13] and

(1) Fowler, J. S.; Wolf, A. P. In *Annual Reports In Medicinal Chemistry*; Allen, R. C. Ed.; Academic Press, Inc.: New York, **1989-24**, p 277.
(2) Jacobson, H. G. *JAMA* **1988**, *259*, 2438.
(3) Eisenhofer, G.; Goldstein, D. S.; Kopin, I. J. *Clin. Sci.* **1989**, *76*, 171.
(4) Rose, C. P.; Burgess, J. H.; Cousineau, D. *J. Clin. Invest.* **1985**, *76*, 1740.
(5) Fowler, J. S.; MacGregor, R. R.; Ansari, A. N.; Atkins, H. L.; Wolf, A. P. *J. Med. Chem.* **1974**, *17*, 246.
(6) Fowler, J. S.; Wolf, A. P.; Christman, D. R.; MacGregor, R. R.; Ansari, A.; Atkins, H. In *Radiopharmaceuticals*; Subramanian, G., Rhodes, B. A., Cooper, J. F., Sodd, V. J. Eds.; The Society of Nuclear Medicine, Inc.: New York, 1975; p 196.
(7) Mislankar, S. G.; Gildersleeve, D. L.; Wieland, D. M.; Massion, C. C.; Mulholland, G. K.; Toorongian, S. A. *J. Med. Chem.* **1988**, *31*, 362.
(8) Haka, M. A.; Rosenspire, K. C.; Gildersleeve, D. L.; Van Dort, M. E.; Sherman, P. S.; Wieland, D. M. *J. Nucl. Med.* **1989**, *30*, 767.
(9) Wieland, D. M.; Rosenspire, K. C.; Hutchins, G. D.; Dort, M. V.; Rothley, J. M.; Mislankar, S. G.; Lee, H. T.; Massion, C. C.; Gildersleeve, D. L.; Sherman, P. S.; Schwaiger, M. *J. Med. Chem.* **1990**, *33*, 956.
(10) Rosenspire, K. C.; Gildersleeve, D. L.; Massin, C. C.; Mislankar, S. G.; Wieland, D. M. *Nucl. Med. Biol.* **1989**, *16*, 735.
(11) Schwaiger, M.; Kalff, V.; Rosenspire, K.; Haka, M. S.; Molina, E.; Hutchins, G. D.; Deeb, M.; Wolfe, E.; Wieland, D. M. *Circulation* **1990**, 82, 457. Kopin, I. J. *Circulation* **1990**, *82*, 646 (Editorial Viewpoint).
(12) Kirk, K. L.; Cantacuzene, D.; Nimikitpaisan, Y.; McCulloh, D.; Padgett, W. L.; Daly, J. W.; Creveling, C. R. *J. Med. Chem.* **1979**, 22, 1493.

0022-2623/91/1834-0767$02.50/0